

Capillary Action in Scalar Active Matter

Adam Wysocki* and Heiko Rieger[†]

Department of Theoretical Physics and Center for Biophysics, Saarland University, Saarbrücken 66123, Germany



(Received 9 August 2019; published 28 January 2020)

We study the capacity of active matter to rise in thin tubes against gravity and other related phenomena like wetting of vertical plates and spontaneous imbibition, where a wetting liquid is drawn into a porous medium. This capillary action or capillarity is well known in classical fluids and originates from attractive interactions between the liquid molecules and the container walls, and from the attraction of the liquid molecules among each other. We observe capillarity in a minimal model for scalar active matter with purely repulsive interactions, where an effective attraction emerges due to slowdown during collisions between active particles and between active particles and walls. Simulations indicate that the capillary rise in thin tubes is approximately proportional to the active sedimentation length λ and that the wetting height of a vertical plate grows superlinear with λ . In a disordered porous medium the imbibition height scales as $\langle h \rangle \propto \lambda \phi_m$, where ϕ_m is its packing fraction. These predictions are highly relevant for suspensions of sedimenting active colloids or motile bacteria in a porous medium under the influence of a constant force field.

DOI: 10.1103/PhysRevLett.124.048001

Introduction.—Recently, active matter, which consists of particles (motile microorganism or active colloids) that consume nutrients or fuel and convert it into a persistent motion, has received a lot of attention due to its intrinsic out-of-equilibrium character on the microscale [1–3]. The simplest representatives of active matter are spherically symmetric, active Brownian particles (ABPs) without alignment, however, with excluded volume interactions [4,5]. Further representatives of the same class, also called scalar active matter, are, for example, run-and-tumble particles [6,7] and active lattice gas [8–11]. Such systems, although far from equilibrium, are in some sense reminiscent of a passive fluid with attractive interactions [12,13], since ABPs slow down during collisions and effectively attract each other. As a result, ABPs undergo a motility-induced phase separation into a coexisting dense and dilute phase [4,5,14,15]. The same mechanism is responsible for adhesion of ABPs to repulsive walls, an effect called wall accumulation [9,16,17].

The investigation of capillary action, the ability of liquids to rise in thin tubes against gravity, has a long history and goes back to Leonardo da Vinci [18]. Its origin is attractive interactions between the liquid molecules and the container walls and the attraction of the liquid molecules among each other causing surface tension. The height of the liquid column in the tube is governed by the balance between the gain in surface energy and the cost in gravitational energy [18,19]. The classical picture seems to prohibit the appearance of capillarity in systems with purely repulsive interactions, however, scalar active matter displays in some sense an equilibrium behavior [20] of an attractive fluid with an equation of state for the pressure and equality of pressures in coexisting phases [21–23]. Still,

their interfacial properties are contradicting: despite stable liquid-gas interfaces the surface tension was found to be negative [24–26], which is also true for solid-liquid interfaces [27]. Consequently, capillarity and imbibition, which in passive systems are based on surface tension, remain elusive for active systems and were not investigated so far.

The natural habitat for many motile bacteria are porous media, such as soil, tissue, or biofilm. So far the transport properties of active particles in heterogeneous media [28–31] have been studied. But, to our knowledge, the classical experiment of spontaneous imbibition of a liquid into a porous medium [32,33] has not been performed with active fluids up to now.

Model.—Several minimal off-lattice models of isotropic active particles without alignment interaction have been proposed [4,7,13]. Here we use a lattice model of scalar active matter, the so-called active lattice gas (ALG) [8–11,34], which allows for simulation of large systems and can be described by exact hydrodynamic equations on macroscopic scales [11,35].

We consider N particles on a square lattice with $N_x \times N_y = (nL_x) \times (nL_y)$ sites, where $1/n$ corresponds to grid spacing, as explained below. Four types of particles $\sigma_{i_x, i_y} \in \{l, r, u, d\}$ corresponding to particles in a left, right, up, and down moving state can occupy a lattice site (i_x, i_y) with maximum occupation number 1 (corresponding to a hard core interaction), cf. Fig. 1(a). Four subprocesses define the stochastic dynamics of the ALG: (i) Symmetric diffusion: a nearest neighbor pair of sites exchange their state with a rate D . (ii) Self-propulsion: particles jump by one lattice spacing in the direction of their moving state

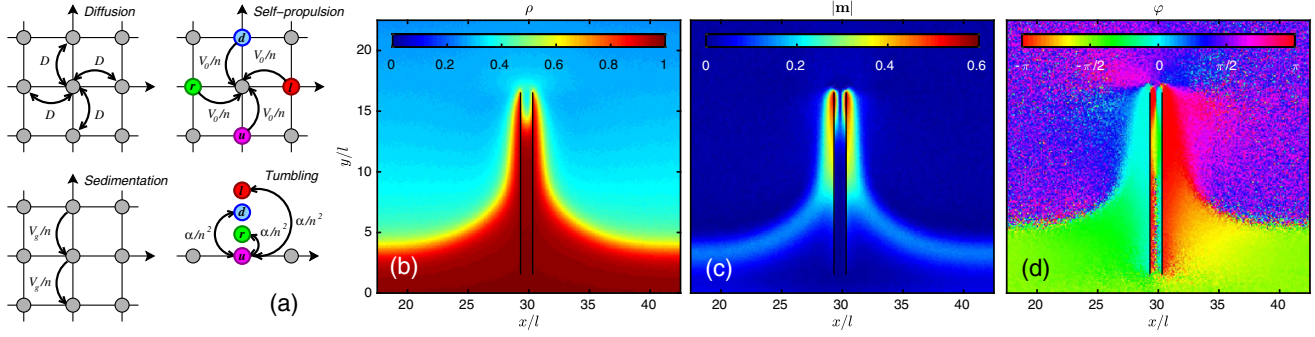


FIG. 1. (a) Sketch of the four subprocesses defining the stochastic dynamics of the ALG: symmetric diffusion, self-propulsion, sedimentation, and tumbling with rates D , V_0/n , V_g/n , and α/n^2 , respectively. (b)–(c) Capillary rise of active lattice gas at active Péclet number $\text{Pe}_a = 10$, gravitational Péclet number $\text{Pe}_g = 0.2$, capillary width $\delta x/l = 1$ and capillary height $\delta y/l = 12.5$. The total size of the system is $L_x/l = 60$ and $L_y/l = 120$, which corresponds to $N_x \times N_y = 1200 \times 2400$ lattice sites used in the Monte Carlo simulation. (b) Mean total density $\rho(x, y) \in [0, 1]$. (c) Absolute value $|\mathbf{m}|(x, y)$ of the mean normalized polarization field \mathbf{m} , see Eq. (2). (d) Phase $\varphi(x, y) \in [-\pi, \pi]$ of $\mathbf{m} = |\mathbf{m}| \cdot (\cos \varphi, \sin \varphi)$. A phase $\varphi = \{0, \pi/2, \{\pi, -\pi\}, -\pi/2\}$ corresponds to a polarization along $\{\hat{x}, \hat{y}, -\hat{x}, -\hat{y}\}$ or $\{\text{right, up, left, down}\}$, respectively.

with a rate V_0/n . (iii) Sedimentation: particles in all moving states jump downward by one lattice spacing with a rate V_g/n . (iv) Tumbling: particles switch state with a rate α/n^2 . Walls are represented as occupied lattice sites, excluding transitions of particles to these sites. Further details can be found in the Supplemental Material [36].

The stochastic process defined in this way generates interacting persistent random walks [10,37] that exhibit a motility-induced phase separation at a critical activity and density as a result of excluded volume interactions [10,11]. We analyze this ALG model numerically by using Monte Carlo (MC) simulations and by the corresponding hydrodynamic equations. Here we only present MC results, which agree quantitatively with the predictions of the hydrodynamic theory as demonstrated in the Supplemental Material [36]. The system has two important dimensionless scaling variables: the active $\text{Pe}_a = V_0/\sqrt{D\alpha}$ and gravitational Péclet number $\text{Pe}_g = V_g/\sqrt{D\alpha}$, which compare either active swimming or gravitation-induced drift motion to thermal diffusion. We use $l = \sqrt{D/\alpha}$ as a length scale.

Our basic setup to study capillarity consists of an ALG confined between horizontal walls at $y = 0$ and $y = L_y$; we apply periodic boundary conditions along the x direction and gravity acts along the negative y direction. As a consequence, a dense phase covers the lower wall with a dilute phase on top of it. The density profile of the dilute phase decays exponentially as $\rho(y) \propto \exp(-y/\lambda)$, where λ is the active sedimentation length, which scales as

$$\lambda \propto V_0^2/\alpha V_g \quad (1)$$

for large activity Pe_a [7,38–40], as has been confirmed by our simulations. In the absence of gravity active particles would accumulate symmetrically at both walls and in the case of an ideal ALG at large Pe_a the density profile, for instance, at the lower wall $y = 0$ would decay as

$\rho(y) \propto C_1 \exp(-y/\lambda_1) + C_2 \exp(-y/\lambda_2)$ with $\lambda_1 = D/V_0$ and $\lambda_2 = \sqrt{D/2\alpha}$, which can be calculated exactly using the corresponding hydrodynamic equations [36].

We insert a capillary or a porous matrix into the dense phase (or confine the system along the x direction by vertical walls), let the system evolve until steady state is reached and adjust simultaneously the number of particles in order to fix the height of the interface between the dense and the dilute phase in the bulk region (far away from perturbations due to vertical walls or porous matrix). We define the position of the interface as the isodensity curve $\rho(x, y) = 0.6$, where $\rho = \rho_l + \rho_r + \rho_u + \rho_d$ is the total density, and fix the height of the interface in the bulk region in all simulations to $y_{\text{bulk}}/l = 4$. In the following, we measure heights, e.g., the height of the meniscus Δh in case of capillary rise, relative to y_{bulk} . We choose the size of the system, such that L_x and L_y are much larger than any other length scale in system, like swimming persistence length V_0/α or active sedimentation length λ . A bulk ALG (no walls) does not phase separate below a critical value $\text{Pe}_a^c = 8$ [41].

Capillary rise.—A typical result for a thin tube and at sufficiently high Pe_a and small Pe_g is shown in Fig. 1 with the mean total density $\rho(x, y) \in [0, 1]$ in Fig. 1(b), the absolute value of the mean normalized polarization field

$$\mathbf{m} = \begin{pmatrix} m_x \\ m_y \end{pmatrix} = \frac{1}{\rho} \begin{pmatrix} \rho_r - \rho_l \\ \rho_u - \rho_d \end{pmatrix} \quad (2)$$

in Fig. 1(c) and the phase $\varphi(x, y) \in [-\pi, \pi]$ of $\mathbf{m} = |\mathbf{m}| \cdot (\cos \varphi, \sin \varphi)$ in Fig. 1(d), which indicates the direction of the polarization \mathbf{m} . The ALG wets the walls of the tube accompanied by a strong polarization in the direction antiparallel to the surface normal, the dense phase fills the tube about the level of the bulk and a concave meniscus develops within the tube. Accumulation at boundaries [9,17,42] and capillary condensation in slit pores [43,44]

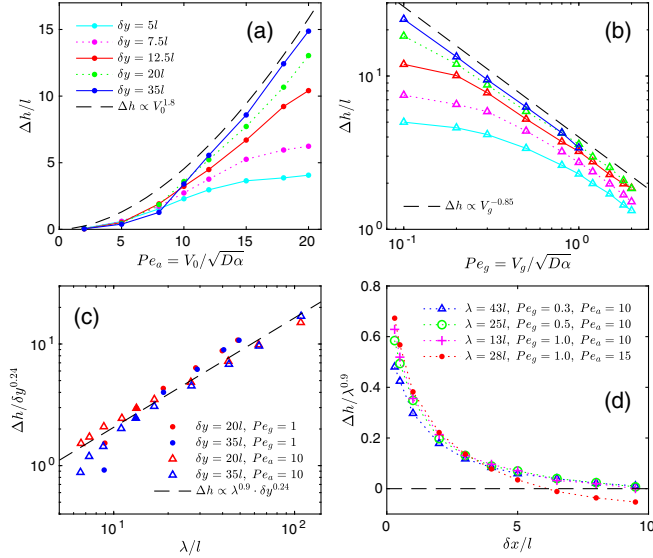


FIG. 2. (a)–(c) The height of the meniscus Δh for different tube heights δy and at a fixed capillary width $\delta x/l = 1$. (a) Δh vs activity Pe_a at fixed $Pe_g = 1$ and (b) Δh vs gravity Pe_g at fixed $Pe_a = 10$. (c) A master curve merging data from (a) and (b). Δh is plotted as a function of active gravitational length λ and Δh is scaled by $\delta y^{0.24}$. For every parameter pair (Pe_a, Pe_g) we estimate the corresponding λ from a fit of the density profile in the bulk. Note that, at finite activity λ is larger than the gravitational length in equilibrium $\lambda_{eq} = D/V_g$. (d) Δh as a function of the capillary width δx for different parameter pairs (Pe_a, Pe_g) and at fixed tube height $\delta y/l = 17.5$. The height of the meniscus Δh is scaled by $\lambda^{0.9}$.

are a well-known effect in scalar active matter; what is new is the rise of the dense phase inside the tube against gravity.

Figures 2(a) and 2(b) illustrate the dependence of the height of the meniscus Δh on activity Pe_a and gravity Pe_g at fixed capillary width $\delta x/l = 1$. As intuitively expected, Δh increases with activity and decreases with gravity. Moreover, Δh increases strongly with the tube height δy until some critical value and saturates above it. In the latter regime we observe an approximate scaling $\Delta h \propto V_0^{1.8}$ and $\Delta h \propto V_g^{-0.85}$. For every parameter pair (Pe_a, Pe_g) we estimate the corresponding active gravitational length λ from a fit of the density profile $\rho(y)$ in the bulk (far away from the tube) to $\rho(y) \propto \exp(-y/\lambda)$. Using this, we obtain a master curve from data shown in Figs. 2(a) and 2(b) by plotting Δh as a function of λ and rescaling Δh for different tube heights by $\delta y^{0.24}$. As indicated in Fig. 2(c) we obtain a simple scaling relation as a result:

$$\Delta h \propto \lambda^{0.9}. \quad (3)$$

The meniscus height Δh decreases strongly with increasing capillary width δx , see Fig. 2(d), and the curves for different pairs (Pe_a, Pe_g) collapse after rescaling of Δh with $\lambda^{0.9}$, which is consistent with the master curve $\Delta h \propto \lambda^{0.9}$ in Fig. 2(c). For large Pe_a and δx the data collapse is not perfect, where Δh even becomes negative.

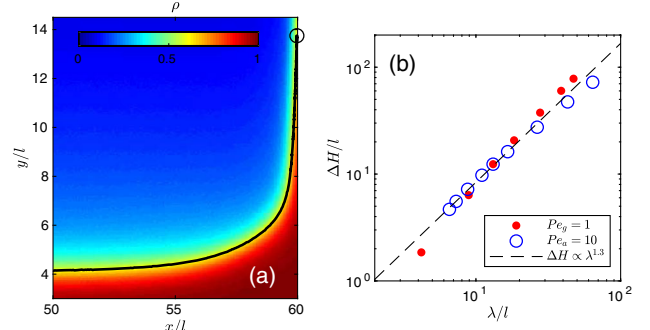


FIG. 3. Wetting of a vertical plate. (a) Total density $\rho(x, y) \in [0, 1]$ for $Pe_a = 10$ and $Pe_g = 1$. A cutout of a larger system ($L_x/l = 60$ and $L_y/l = 120$) is shown. Black line indicates the isodensity at $\rho = 0.6$, which is our definition of the interface between the dense and the dilute phase. The height of the wetting layer ΔH is marked by a circle. (b) Height of the wetting layer ΔH as a function of the active gravitational length λ . Two datasets are shown: $2 \leq Pe_a \leq 20$ at fixed $Pe_g = 1$ and $0.1 \leq Pe_g \leq 2$ at fixed $Pe_a = 10$.

Wetting of a vertical plate.—As mentioned above, the dense phase of the ALG not only rises inside a capillary but also wets the outside walls of the capillary. In order to study the latter effect separately we consider a setup of a rectangular container with horizontal walls at $y = 0$ and $y = L_y$ and vertical walls at $x = 0$ and $x = L_x$. Again we adjust the number of particles in order to fix the height of the interface far away from walls ($x = L_x/2$). A typical total density field $\rho(x, y) \in [0, 1]$ together with the isoline at $\rho = 0.6$ (definition of the interface) is shown in Fig. 3(a), where a pronounced wetting of the vertical wall is visible. We estimate the height of the wetting layer ΔH for different parameter pairs (Pe_a, Pe_g) together with the corresponding active gravitational lengths λ and obtain a master curve, which suggests a superlinear growth,

$$\Delta H \propto \lambda^{1.3}, \quad (4)$$

of the wetting height. Phenomenologically, wetting can here be understood as follows: activity leads to an accumulation of particles at the container walls and gravity forces particles to sediment to the bottom. However, excluded volume effect prevents a collapse of the wetting layer. A zero-order approximation for the interface profile in a capillary tube of a width δx is a superposition of wetting profiles of two independent walls at distance δx .

Imbibition of a porous matrix.—Motivated by the above results we probe now how the ALG penetrates a porous medium. We construct a porous matrix from randomly placed nonoverlapping hard discs with uniformly distributed diameters in the range $\sigma/l \in [0.5, 2]$ and a minimum gap size of $0.325l$. As in the previous setups, we adjust the number of particles in order to fix the interface far away from the matrix. An example of a spontaneous imbibition is

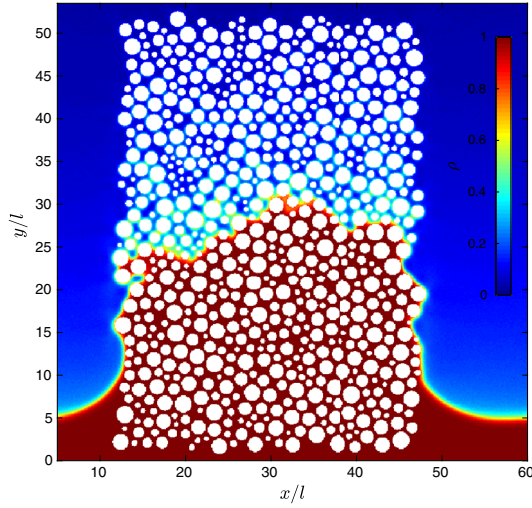


FIG. 4. Imbibition of a porous media by the active lattice gas. The porous media consists of nonoverlapping hard discs with uniformly distributed diameters in the range $\sigma/l \in [0.5, 2]$; the minimum gap size is 0.325 in units of l . The total density $\rho(x, y) \in [0, 1]$ is shown for $Pe_a = 15$, $Pe_g = 1$ and a system size $L_x/l = 60$ and $L_y/l = 100$. The porosity is $1 - \phi_m = 0.2$, where ϕ_m is the packing fraction of the porous matrix.

shown in Fig. 4 for a matrix packing fraction of $\phi_m = 0.8$ (i.e., porosity 0.2). After an initial rise the invasion front reaches a final height and width, and the interface fluctuates slightly in the steady state.

An obvious question is: What is the effect of the porosity on the imbibition? In Fig. 5(a) we present the average density profiles $\rho(y)$ of the active lattice gas within the porous matrix for different porosities $1 - \phi_m$ at $(Pe_a, Pe_g) = (15, 1)$ and indicate the position of the interface by circles; the horizontal average was performed over the void region only and over 10 independent realizations of the matrix. As expected, the smaller the porosity the higher the rise of the dense phase within the porous matrix. Interestingly, the density of the dilute phase above the invasion front within the matrix is significantly larger than the bulk density at the same height, see dashed line in Fig. 5(a).

We perform similar simulations for different (Pe_a, Pe_g) and estimate the mean interface height $\langle h \rangle$ and the corresponding active gravitational length λ . A scaling of $\langle h \rangle$ with λ leads to a reasonable data collapse and indicates a simple growth relation

$$\langle h \rangle \propto \lambda \phi_m \quad (5)$$

of the interface height; see Fig. 5(b). A rough comparison between imbibition and capillary rise can be done by plotting together the mean interface height $\langle h \rangle$ vs mean gaps size of the porous matrix, obtained with Delaunay triangulation, and the height of the meniscus Δh vs capillary width δx , see Fig. 2(d). Although the shape of the curves is similar, the capacity of ALG to rise in porous media against

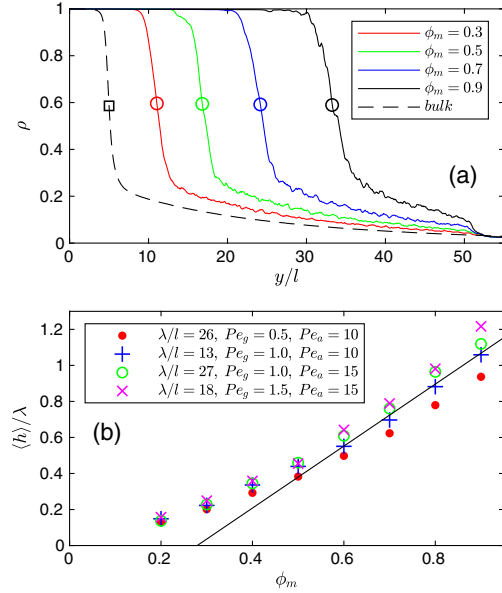


FIG. 5. (a) Density profiles $\rho(y)$ of the active lattice gas within the porous matrix (the horizontal average was performed over the void region only) for different porosities $1 - \phi_m$ (solid lines) and the corresponding $\rho(y)$ in the bulk region (dashed line) are shown. The position of the interface is defined as the height, where $\rho = 0.6$ and is indicated by circles for the porous matrix and by a square in the bulk. The parameters are $(Pe_a, Pe_g) = (15, 1)$. (b) Mean interface height $\langle h \rangle$ scaled by the active gravitational length λ as a function of the packing fraction of the porous matrix ϕ_m for different parameter pairs (Pe_a, Pe_g) .

the action of gravity is twice as strong as in thin tubes and the reason for this is that the porous matrix contains also gap sizes much smaller than the average.

Conclusions and outlook.—We have shown that scalar active matter with purely repulsive interactions can rise in thin tubes or invade porous matrix against gravity. As a proof of concept we have used one of the simplest active matter models and there are several obvious extensions in the study of active capillarity and related phenomena using more realistic and elaborated models. It is obvious to consider next off-lattice models, such as active Brownian particles (ABPs), in order to test the universality of the scaling relations; preliminary simulations clearly demonstrate capillary action in ABPs and confirm the robustness of the effect in active matter systems [45]. Hydrodynamic interactions [46,47] or, in the case of anisotropic active particles, alignment interactions can have a dramatic effect on the behavior near boundaries as compared to scalar active matter and should be taken into account in future studies. It would be very interesting to investigate the modification of classical capillary rise [48] by activity using active colloids with attraction [49], where it is predicted that wall attraction may cause capillary drying [44]. Also the study of capillary action and wetting in active multiphase systems, such as suspensions of motile bacteria [50], algae [51], or synthetic self-propelled particles [52,53]

is very promising and could be a possible experimental test for our predictions.

This work was financially supported by the German Research Foundation (DFG) within the Collaborative Research Center SFB 1027. We thank Matthieu Mangiat for introduction into FreeFEM, Reza Shaebani for careful proofreading, Sergej Rjasanow and Steffen Weißer for tips about numerical methods.

*a.wysocki@lusi.uni-sb.de

†h.rieger@mx.uni-saarland.de

- [1] M. C. Marchetti, J. F. Joanny, S. Ramaswamy, T. B. Liverpool, J. Prost, M. Rao, and R. A. Simha, Hydrodynamics of soft active matter, *Rev. Mod. Phys.* **85**, 1143 (2013).
- [2] J. Elgeti, R. G. Winkler, and G. Gompper, Physics of microswimmers—single particle motion and collective behavior: A review, *Rep. Prog. Phys.* **78**, 056601 (2015).
- [3] M. Reza Shaebani, A. Wysocki, R. G. Winkler, G. Gompper, and H. Rieger, Computational models for active matter, [arXiv:1910.02528](https://arxiv.org/abs/1910.02528).
- [4] Y. Fily and M. C. Marchetti, Athermal Phase Separation of Self-Propelled Particles with No Alignment, *Phys. Rev. Lett.* **108**, 235702 (2012).
- [5] G. S. Redner, M. F. Hagan, and A. Baskaran, Structure and Dynamics of a Phase-Separating Active Colloidal Fluid, *Phys. Rev. Lett.* **110**, 055701 (2013).
- [6] J. Tailleur and M. E. Cates, Statistical Mechanics of Interacting Run-and-Tumble Bacteria, *Phys. Rev. Lett.* **100**, 218103 (2008).
- [7] A. P. Solon, M. E. Cates, and J. Tailleur, Active Brownian particles and run-and-tumble particles: A comparative study, *Eur. Phys. J. Spec. Top.* **224**, 1231 (2015).
- [8] A. G. Thompson, J. Tailleur, M. E. Cates, and R. A. Blythe, Lattice models of nonequilibrium bacterial dynamics, *J. Stat. Mech.* (2011) P02029.
- [9] N. Sepúlveda and R. Soto, Wetting Transitions Displayed by Persistent Active Particles, *Phys. Rev. Lett.* **119**, 078001 (2017).
- [10] S. Whitelam, K. Klymko, and D. Mandal, Phase separation and large deviations of lattice active matter, *J. Chem. Phys.* **148**, 154902 (2018).
- [11] M. Kourbane-Houssene, C. Erignoux, T. Bodineau, and J. Tailleur, Exact Hydrodynamic Description of Active Lattice Gases, *Phys. Rev. Lett.* **120**, 268003 (2018).
- [12] M. E. Cates and J. Tailleur, Motility-induced phase separation, *Annu. Rev. Condens. Matter Phys.* **6**, 219 (2015).
- [13] T. F. F. Farage, P. Krinninger, and J. M. Brader, Effective interactions in active Brownian suspensions, *Phys. Rev. E* **91**, 042310 (2015).
- [14] J. Stenhammar, D. Marenduzzo, R. J. Allen, and M. E. Cates, Phase behaviour of active Brownian particles: The role of dimensionality, *Soft Matter* **10**, 1489 (2014).
- [15] A. Wysocki, R. G. Winkler, and G. Gompper, Cooperative motion of active Brownian spheres in three-dimensional dense suspensions, *Europhys. Lett.* **105**, 48004 (2014).
- [16] C. F. Lee, Active particles under confinement: Aggregation at the wall and gradient formation inside a channel, *New J. Phys.* **15**, 055007 (2013).
- [17] J. Elgeti and G. Gompper, Wall accumulation of self-propelled spheres, *Europhys. Lett.* **101**, 48003 (2013).
- [18] P.-G. De Gennes, F. Brochard-Wyart, and D. Quéré, *Capillarity and Wetting Phenomena: Drops, Bubbles, Pearls, Waves* (Springer Science & Business Media, New York, 2013).
- [19] J. S. Rowlinson and B. Widom, in *Molecular Theory of Capillarity*, Dover Books on Chemistry (Dover Publications, Mineola, New York, 2013).
- [20] É. Fodor, C. Nardini, M. E. Cates, J. Tailleur, P. Visco, and F. van Wijland, How Far From Equilibrium is Active Matter?, *Phys. Rev. Lett.* **117**, 038103 (2016).
- [21] A. P. Solon, Y. Fily, A. Baskaran, M. E. Cates, Y. Kafri, M. Kardar, and J. Tailleur, Pressure is not a state function for generic active fluids, *Nat. Phys.* **11**, 673 (2015).
- [22] A. P. Solon, J. Stenhammar, R. Wittkowski, M. Kardar, Y. Kafri, M. E. Cates, and J. Tailleur, Pressure and Phase Equilibria in Interacting Active Brownian Spheres, *Phys. Rev. Lett.* **114**, 198301 (2015).
- [23] S. Das, G. Gompper, and R. G. Winkler, Local stress and pressure in an inhomogeneous system of spherical active Brownian particles, *Sci. Rep.* **9**, 6608 (2019).
- [24] J. Bialké, J. T. Siebert, H. Löwen, and T. Speck, Negative Interfacial Tension in Phase-Separated Active Brownian Particles, *Phys. Rev. Lett.* **115**, 098301 (2015).
- [25] A. Patch, D. M. Sussman, D. Yllanes, and M. C. Marchetti, Curvature-dependent tension and tangential flows at the interface of motility-induced phases, *Soft Matter* **14**, 7435 (2018).
- [26] A. P. Solon, J. Stenhammar, M. E. Cates, Y. Kafri, and J. Tailleur, Generalized thermodynamics of motility-induced phase separation: Phase equilibria, laplace pressure, and change of ensembles, *New J. Phys.* **20**, 075001 (2018).
- [27] R. Zakine, Y. Zhao, M. Knežević, A. Daerr, Y. Kafri, J. Tailleur, and F. van Wijland, Surface tensions between active fluids and solid interfaces: Bare vs dressed, [arXiv:1907.07738](https://arxiv.org/abs/1907.07738).
- [28] O. Chepizhko, E. G. Altmann, and F. Peruani, Optimal Noise Maximizes Collective Motion in Heterogeneous Media, *Phys. Rev. Lett.* **110**, 238101 (2013).
- [29] C. Reichhardt and C. J. Olson Reichhardt, Active matter transport and jamming on disordered landscapes, *Phys. Rev. E* **90**, 012701 (2014).
- [30] E. Pinçe, S. K. P. Velu, A. Callegari, P. Elahi, S. Gigan, G. Volpe, and G. Volpe, Disorder-mediated crowd control in an active matter system, *Nat. Commun.* **7**, 10907 (2016).
- [31] R. Alonso-Matilla, B. Chakrabarti, and D. Saintillan, Transport and dispersion of active particles in periodic porous media, *Phys. Rev. Fluids* **4**, 043101 (2019).
- [32] M. Alava, M. Dub, and M. Rost, Imbibition in disordered media, *Adv. Phys.* **53**, 83 (2004).
- [33] S. Gruener, Z. Sadjadi, H. E. Hermes, A. V. Kityk, K. Knorr, S. U. Egelhaaf, H. Rieger, and P. Huber, Anomalous front broadening during spontaneous imbibition in a matrix with elongated pores, *Proc. Natl. Acad. Sci. U.S.A.* **109**, 10245 (2012).

- [34] A. Manacorda and A. Puglisi, Lattice Model to Derive the Fluctuating Hydrodynamics of Active Particles with Inertia, *Phys. Rev. Lett.* **119**, 208003 (2017).
- [35] A. De Masi, P. A. Ferrari, and J. L. Lebowitz, Rigorous Derivation of Reaction-Diffusion Equations with Fluctuations, *Phys. Rev. Lett.* **55**, 1947 (1985).
- [36] See Supplemental Material at <http://link.aps.org/supplemental/10.1103/PhysRevLett.124.048001> for a detailed definition of the stochastic processes and a sketch illustrating these rules. The microscopic equations for the average occupation number and macroscopic equations for the density are provided. MC simulation results are compared to numerical solutions of the macroscopic equations.
- [37] T. Bertrand, Y. Zhao, O. Bénichou, J. Tailleur, and R. Voituriez, Optimized Diffusion of Run-and-Tumble Particles in Crowded Environments, *Phys. Rev. Lett.* **120**, 198103 (2018).
- [38] J. Tailleur and M. E. Cates, Sedimentation, trapping, and rectification of dilute bacteria, *Europhys. Lett.* **86**, 60002 (2009).
- [39] M. Enculescu and H. Stark, Active Colloidal Suspensions Exhibit Polar Order Under Gravity, *Phys. Rev. Lett.* **107**, 058301 (2011).
- [40] F. Ginot, A. Solon, Y. Kafri, C. Ybert, J. Tailleur, and C. Cottin-Bizonne, Sedimentation of self-propelled janus colloids: Polarization and pressure, *New J. Phys.* **20**, 115001 (2018).
- [41] M. Mangeat (private communication).
- [42] T. Ostapenko, F. Jan Schwarzendahl, T. J. Bøddeker, C. Titus Kreis, J. Cammann, M. G. Mazza, and O. Bäumchen, Curvature-Guided Motility of Microalgae in Geometric Confinement, *Phys. Rev. Lett.* **120**, 068002 (2018).
- [43] R. Ni, M. A. Cohen Stuart, and P. G. Bolhuis, Tunable Long Range Forces Mediated by Self-Propelled Colloidal Hard Spheres, *Phys. Rev. Lett.* **114**, 018302 (2015).
- [44] R. Wittmann and J. M. Brader, Active Brownian particles at interfaces: An effective equilibrium approach, *Europhys. Lett.* **114**, 68004 (2016).
- [45] A. Wysocki and H. Rieger (to be published).
- [46] K. Drescher, J. Dunkel, L. H. Cisneros, S. Ganguly, and R. E. Goldstein, Fluid dynamics and noise in bacterial cell-cell and cell-surface scattering, *Proc. Natl. Acad. Sci. U.S.A.* **108**, 10940 (2011).
- [47] V. Kantsler, J. Dunkel, M. Polin, and R. E. Goldstein, Ciliary contact interactions dominate surface scattering of swimming eukaryotes, *Proc. Natl. Acad. Sci. U.S.A.* **110**, 1187 (2013).
- [48] D. I. Dimitrov, A. Milchev, and K. Binder, Capillary Rise in Nanopores: Molecular Dynamics Evidence for the Lucas-Washburn Equation, *Phys. Rev. Lett.* **99**, 054501 (2007).
- [49] G. S. Redner, A. Baskaran, and M. F. Hagan, Reentrant phase behavior in active colloids with attraction, *Phys. Rev. E* **88**, 012305 (2013).
- [50] E. Lauga, Bacterial hydrodynamics, *Annu. Rev. Fluid Mech.* **48**, 105 (2016).
- [51] R. E. Goldstein, Green algae as model organisms for biological fluid dynamics, *Annu. Rev. Fluid Mech.* **47**, 343 (2015).
- [52] J. Palacci, S. Sacanna, A. P. Steinberg, D. J. Pine, and P. M. Chaikin, Living crystals of light-activated colloidal surfers, *Science* **339**, 936 (2013).
- [53] I. Buttinoni, J. Bialké, F. Kümmel, H. Löwen, C. Bechinger, and T. Speck, Dynamical Clustering and Phase Separation in Suspensions of Self-Propelled Colloidal Particles, *Phys. Rev. Lett.* **110**, 238301 (2013).